The effects of friction stir welding on the mechanical properties and microstructure of 7000 series aluminium tailor-welded blanks

A.A. Zadpoor[1,2], J. Sinke[2], R. Benedictus[2]

[1]*Netherlands Institute for Metals Research – Mekelweg 2, Delft 2628CD, Delft, The Netherlands*
URL: www.nimr.nl *e-mail: A.A.Zadpoor@tudelft.nl*

[2]*Faculty of Aerospace Engineering, Delft University of Technology (TU Delft)- Kluyverweg 1, Delft 2629HS, The Netherlands*
URL: www.vm.lr.tudelft.nl *e-mail: J. Sinke@ tudelft.nl; R.Benedictus@tudelft.nl*

ABSTRACT: The mechanical properties and microstructure of Friction Stir Welded (FSW) tailor made blanks from 7000 series alloys is studied in this paper. The 7075-T6 alloy is selected for the study and three different thicknesses of this alloy are welded together to make tailor-made blanks with three different thickness ratios, i.e. 1, 1.3, and 1.7. The microstructure, hardness profile, global mechanical properties (in as-welded and machined conditions), and local mechanical properties (captured by Digital Image Correlation (DIC) method) of the welds are presented. It has been shown that though in all cases the strength and formability of the welded blanks are lower than those of the base metals, other factors such as the thickness ratio play an important role in this regard.

Key words: Friction stir welding, microstructure, hardness profile, global and local mechanical properties

1 INTRODUCTION

Increasing demand for lighter, more fuel-efficient, and cleaner vehicles has boosted new manufacturing technologies such as Tailor-Welded Blanks (TWBs) which aim at lightening the vehicular structures through optimal structural design, application of advanced materials, or, as in the case of tailor-made blanks, optimal distribution of material within the structural parts. TWBs are sheet metals with possibly different thicknesses and/or materials which are welded together prior to the forming. The possibility of having different thicknesses and materials in a single assembly facilitates the optimal material distribution. Tailor-welded blanks have found numerous applications in the automotive industry. However, their applications are very limited in the aircraft industry primarily due to the high welding temperatures of the conventional welding processes which adversely affect the mechanical properties of the 2000 and 7000 series high strength aluminium alloys. Therefore, new welding techniques are needed in order to make tailor-welded blanks in the aircraft industry. Friction Stir Welding (FSW) is a solid state joining process which can be used for this purpose. In the case of FSW, the welding temperatures are well below the melting temperature hence minimizing the adverse effects of the welding process. Nevertheless, the microstructure and, thus, the mechanical properties of the sheets are affected by the welding process. In this paper, the effects of FSW on the microstructure and mechanical properties of 7000 series aluminium TWBs are studied to understand how they affect the formability of FSW TMBs. The 7075-T6 alloy which is commonly used in the aircraft structures is selected for the study. Three different thicknesses are used for welding. For each welded series, a parametric study is conducted such that the welding parameters can be optimized as good as possible. The microstructural features, hardness profiles, and global/local mechanical properties of the welds are studied. The effects of the thickness ratio on the mechanical properties and microstructural features are investigated. It has been shown that albeit always lower than those of the base metals, the strength and formability of the tailor-welded blanks are heterogeneously distributed within the blanks and are dependent on the thickness ratio.

2 MATERIALS AND METHODS

2.1 Materials

Three different thicknesses of 7075-T6 sheets, as listed in Table 1, were used to make the welds. The resulting thickness ratios varied between 1 and 1.7. The mechanical properties of the base metals vary from one thickness to the other. Therefore, it was necessary to characterize each batch separately. Six samples from each batch of the base materials were tested. The results of the tensile testing are given in Table 2.

Table 1. The weld configurations studied in this paper

no.	material I	t_1 (mm)	material II	t_2 (mm)	t_1/t_2
1	7075-T6	2.0	7075-T6	2.0	1.0
2	7075-T6	2.0	7075-T6	1.2	1.7
3	7075-T6	2.5	7075-T6	2.0	1.3

Table 2. The mechanical properties of the base metals

material	t (mm)	σ_y (MPa)	σ_{max} (MPa)	ε_{Fmax} (%)
7075-T6	2.0	533±2	585±2	11.9±0.2
7075-T6	1.2	556±1	595±2	10.8±0.4
7075-T6	2.5	554±1	589±1	10.8±0.1

2.2 Welding procedure

A Cartesian ESAB Superstir FSW machine was used for production of the welds. The rolling direction of the sheets was in parallel with the welding direction. Two different welding angles were used. First, the welding angle (tool angle), α, which is the angle of the welding tool with the blanks in the direction of the welding (see Figure 1a). The second welding angle (inclination angle), θ, is the angle of the tool with the workpiece in the direction perpendicular to the welding direction. The head of the FSW machine was rotated to create a tool angle (α) of 2 degrees. The same tool angle was used for all the configurations listed in Table 1. The inclination angle was generated by tilting the clamping assembly. Figure 1b shows the clamping used to generate the inclination angle. The inclination angle was used only for configurations number 2 and 3. For each configuration, the inclination angle was determined during the parametric study (as described in the next section).

2.3 Parametric study

Since the mechanical properties of the welds are highly dependent on the welding parameters, it is necessary to determine the welding parameters. Ideally, one would want to use optimal welding parameters not only because that would lead to the best welds but also because that would facilitate the comparative study between different weld configurations.

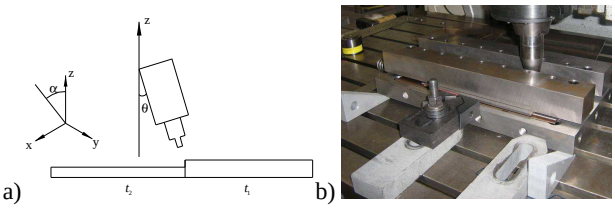

Fig. 1. A schematic drawing (a) and a picture (b) of the weld setup illustrating the inclination and tool angles

The final weld parameters were selected based on the parametric study and are listed in Table 3. The welds, for each configuration, were produced by using these parameters. After welding, the welds were naturally aged for a minimum of 45 days to ensure optimal mechanical properties.

Table 3. The welding parameters determined through the parametric study

parameter	series 1	series 2	series 3
α	2^o	2^o	2^o
θ	0	2.1^o	2.1^o
shoulder diam. (mm)	12	13	13
pin diam. (mm)	5	5	5
rot speed (min^{-1})	400	400	400
travel speed (mm/min)	100	100	100

2.4 Experiments

Four sets of tests were carried out on the weld samples: metallography, hardness measurement, tensile testing, and fractography. The samples for the metallographic study were mounted, ground, and polished up to 1μm. Subsequently, the samples were electrochemically etched by using a Baker etching agent and an optical microscope with digital camera, polarization filter, and ¼ lambda filter was used to study the microstructure of the samples. The hardness profiles of the welds were determined by using an automatic micro-indenter. A fixed load of 200g was applied and the distance between indentations was set at 0.4 mm. The tensile test was carried out in as-welded and machined conditions. The as-welded samples were cut and machined to the standard (ASTM E8) dog bone shape. The top surface of the machined samples was machined to obtain a thickness uniform throughout the specimen. The loading direction of the samples was

perpendicular to the welding direction. The tests were carried out by using a Zwick/Roell static test machine and a constant rate of 3 mm/min. The surface of the machined specimens was covered with a random ink pattern and the deformation of the samples during the test was captured by using a high frame rate digital camera. The pictures were analyzed by an in-house-developed Digital Image Correlation (DIC) code to calculate the local strain values. After the tensile testing, the fracture surfaces of the specimens were analyzed by Scanning Electron Microscopy (SEM).

3 RESULTS

Figure 2 shows the boundary between the weld nugget and TMAZ (ThermoMechanically-Affected Zone)/HAZ (Heat-Affected Zone) for one sample weld from configuration number 1. The hardness profile of this sample at the centreline of the weld cross section is depicted in Figure 3. The average values and standard deviations of the true yield and tensile strengths and the true global strains at the maximum stress resulting from the tensile tests are listed in Table 4. The fracture surface of one sample specimen is shown in Figures 4a and 4b. The results of the DIC strain analysis of the machined tensile test specimens are presented in Figures 5 to 7. Figures 5 and 6 show the local yield strength and the local values of the strain hardening exponent around the weld centreline, respectively. Figure 7 depicts the local stress-strain curves and variation of the local yield strength values around the weld centreline from the advancing to the retreating side.

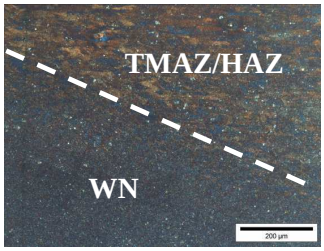

Fig. 2. Microstructure and boundary between the different zones of a sample weld from configuration number 1

4 DISCUSSIONS

Metallographic analysis showed that the thermo-mechanical processing of the sheets during FSW has significantly changed the microstructure of the sheets. The grains were found to be highly refined in the weld nugget. There was also a TMAZ with highly distorted grain shapes which by progressing to the sides of the weld vanished to let the normal morphology of the sheet reappear. The fracture surfaces showed a combined ductile and brittle fracture. However, the dimple-shape structure and tearing edges which are typical for the ductile fracture predominantly occupied the fracture surface leaving less space for the brittle-shape fracture in the fracture surface.

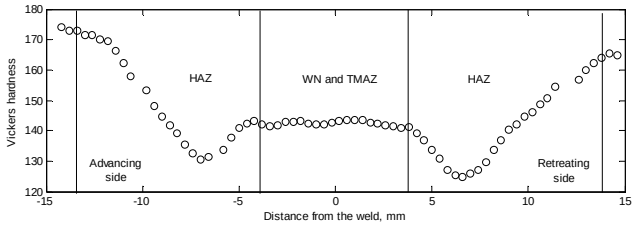

Fig. 3. Hardness profile of a weld from configuration number 1

Table 4. The mechanical properties of the as-welded and machined specimens

parameter		series 1	series 2	series 3
σ_y (MPa)	as-welded	442±9	421±4	428±1
	machined	401±8	384±10	378±11
σ_{max} (MPa)	as-welded	551±4	449±3	510±4
	machined	519±9	514±15	502±12
ε_{Fmax} (%)	as-welded	9.3±0.3	4.0±0.5	5.9±0.0
	machined	7.7±0.2	7.1±0.2	7.9±0.2
Failure location	as-welded	HAZ	HAZ	HAZ
	machined	HAZ	HAZ	HAZ

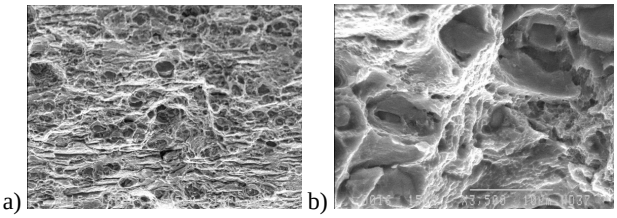

Fig. 4. Fracture surface of a sample specimen with 500x (a) and 3500x (b) magnifications

As is clear from the results, the mechanical properties of the welded sheets are quite heterogeneous. The dynamic recrystallization has resulted in a very fine grain structure in the weld nugget, which suffers from softening (see Figure 3). The softest zone, however, corresponds to the HAZ where the mechanical properties are diminished merely because of the thermal effects without involvement of the mechanical evolution which influences the other places such as the weld nugget and TMAZ.

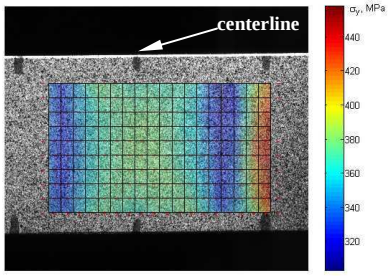

Fig. 5. Local yield strength values around the weld centreline

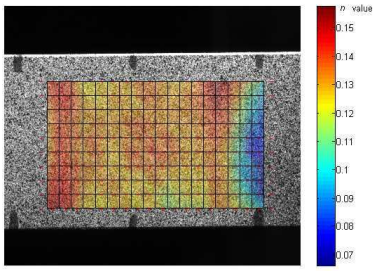

Fig. 6. Local values of the strain hardening exponent around the weld centreline

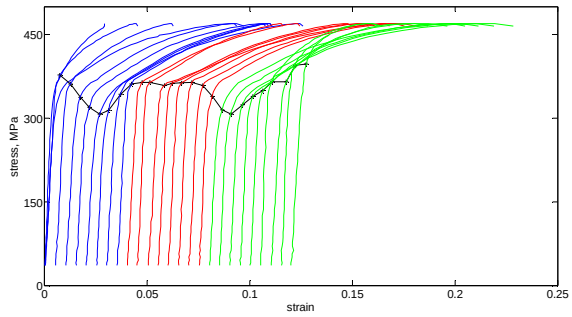

Fig. 7. The local stress-strain curves and the yield strengths from the advancing to the retreating sides of a sample weld

The failure always occurs in the HAZ regardless of the thickness ratio and the specimen being tested as-welded or in the machined condition. Therefore, it is important to design the sheet metal forming process such that this area does not undergo large strains. Table 4 shows that for all configurations, the yield and tensile strengths as well as the strains at the maximum stress decrease after the welding. An important point is the effect of the thickness ratio on the mechanical properties of the welds. In almost all cases, the mechanical properties decrease as the thickness ratio increases. The effect of machining on the mechanical properties is two folds. On one hand, the machining removes the gradual thickness change which influences the strain and stress distribution around the weld nugget. On the other hand, the machining process removes the effects of the welding tool's shoulder which penetrates superficially into the sheets. Because all geometric effects are removed in the machined specimens, the mechanical properties of the welds can be studied independent from the geometric effects. Figures 5 and 6 show that there is a very heterogeneous distribution of the mechanical properties such as the yield strength and strain hardening exponent in the areas close to the weld centerline. This is an important point in view of the fact that the design and simulation of the forming processes would face some additional difficulties because of the complicated distribution of the mechanical properties. The present authors have previously shown that skipping the mechanical properties of the weld nugget and HAZ results in inaccurate prediction of the strain distribution and springback behavior in FEM modeling of FSW TWBs ([1] and [2]). The local stress-strain curves and the yield strengths shown in Figure 7 resemble the pattern of the micro-hardness profile presented in Figure 3. This is an indication of the consistency and relevance of the DIC method and is supportive of the importance of this optical method for measurement of the local mechanical properties of FSW TWBs.

5 CONCLUSIONS

The results of this study show that FSW has a major impact on the microstructure and mechanical properties of FSW TWBs. Of particular importance are the reduced formability and strength and heterogeneity of the properties within the blank. In addition, there are some phenomena which are specific to the welds with dissimilar thicknesses and make the understanding of the behavior of FSW TWBs even more complicated. For example, the thickness ratio significantly affects the properties of the blank.

ACKNOWLEDGEMENTS

This research was carried out under projectnumber MC1.05224 in the framework of the Strategic Research program of the Netherlands Institute for Metals Research in the Netherlands (www.nimr.nl).

REFERENCES

1. AA. Zadpoor, J. Sinke and R. Benedictus, Finite element modelling of transition zone in friction stir welded tailor-made blanks, In: *Proc. NUMIFORM'07*, eds, J.M.A. Cesar de Sa, A.D. Santosa, AIP Conference Proceedings vol. 908 (2007) 1457-1462.
2. AA. Zadpoor, J. Sinke and R. Benedictus, Springback behavior of friction stir welded tailor-made blanks, In: *Proc. IDDRG07*, eds, M. Tisza, Gyor (2007), 317.-324.